

# Exact Excited-State Functionals of the Asymmetric Hubbard Dimer

Sara Giarrusso<sup>1,\*</sup> and Pierre-François Loos<sup>1,†</sup>

<sup>1</sup>Laboratoire de Chimie et Physique Quantiques (UMR 5626), Université de Toulouse, CNRS, UPS, France

We derive, for the case of the asymmetric Hubbard dimer at half-filling, the exact functional associated with each singlet ground and excited state, using both Levy’s constrained search and Lieb’s convex formulation. While the ground-state functional is, as commonly known, a convex function with respect to the density (or, more precisely, the site occupation), the functional associated with the (highest) doubly-excited state is found to be concave. Also, we find that, because the density of the first excited state is non-invertible, its “functional” is a partial, multi-valued function composed of one concave and one convex branch that correspond to two separate sets of values of the external potential. These findings offer insight into the challenges of developing state-specific excited-state density functionals for general applications in electronic structure theory.

*DFT for ground states.*— Density-functional theory (DFT) is a mature theory built on firm and rigorous mathematical knowledge [1]. Originally based on the two Hohenberg-Kohn theorems [2] — known as the pillars of DFT — and its practical Kohn-Sham scheme [3] that makes it the workhorse of electronic structure theory, exact mathematical results and new theoretical developments are usually achieved thanks to Levy’s constrained-search formulation [4]. In particular, the Hohenberg-Kohn variational principle states that, in the case of a ground state, the total energy is given by

$$E_0[v] = \min_{\rho} \left\{ F[\rho] + \int v(\mathbf{r})\rho(\mathbf{r})d\mathbf{r} \right\} \quad (1)$$

or, equivalently, via a Legendre-Fenchel transform, Lieb’s convex formulation of DFT (or the Lieb variational principle) teaches us that the universal density functional is [5]

$$F[\rho] = \max_v \left\{ E[v] - \int v(\mathbf{r})\rho(\mathbf{r})d\mathbf{r} \right\} \quad (2)$$

which puts forward the duality between the concave function  $E_0[v]$  with respect to the external potential  $v$  and  $F[\rho]$ , a convex function of the density  $\rho$  [6]. In other words, these quantities, known as conjugate functions (or Fenchel conjugates), have the same content but different “packaging”.

Levy’s constrained search starts with the usual variational principle

$$E_0[v] = \min_{\Psi} \langle \Psi | \hat{H}_v | \Psi \rangle \quad (3)$$

where the minimization is performed over all normalized  $N$ -electron antisymmetrized wave functions  $\Psi$  and the electronic Hamiltonian

$$\hat{H}_v = \hat{T} + \hat{V}_{ee} + \sum_{i=1}^N v(\mathbf{r}_i) \quad (4)$$

is composed of the kinetic energy operator  $\hat{T}$ , the electron repulsion operator  $\hat{V}_{ee}$ , and the external potential contribution. Following Levy’s seminal work [4], one recasts

the previous equation as

$$E_0[v] = \min_{\rho} \min_{\Psi \rightsquigarrow \rho} \langle \Psi | \hat{H}_v | \Psi \rangle \quad (5)$$

where the notation  $\Psi \rightsquigarrow \rho$  stands for a wave function  $\Psi$  that yields a density  $\rho$ . By defining the universal functional as

$$F[\rho] = \min_{\Psi \rightsquigarrow \rho} \langle \Psi | \hat{H}_0 | \Psi \rangle = \langle \Psi[\rho] | \hat{H}_0 | \Psi[\rho] \rangle \quad (6)$$

we recover the Hohenberg-Kohn variational principle defined in Eq. (1) with  $\hat{H}_0 = \hat{T} + \hat{V}_{ee}$ .

Therefore, within the Hohenberg-Kohn formulation of DFT, for a given  $v(\mathbf{r})$ , we seek the density  $\rho(\mathbf{r})$  such that the following Euler equation is fulfilled

$$\frac{\delta F[\rho(\mathbf{r})]}{\delta \rho(\mathbf{r})} + v(\mathbf{r}) = 0 \quad (7)$$

with  $F[\rho] = T[\rho] + V_{ee}[\rho]$ , the total energy being given by

$$E_0[v] = F[\rho] + \int v(\mathbf{r})\rho(\mathbf{r})d\mathbf{r} \quad (8)$$

with  $T[\rho] = \langle \Psi[\rho] | \hat{T} | \Psi[\rho] \rangle$  and  $V_{ee}[\rho] = \langle \Psi[\rho] | \hat{V}_{ee} | \Psi[\rho] \rangle$ .

*DFT for excited states.*— Accessing excited states at the DFT level usually means resorting to time-dependent DFT (TD-DFT) [7–10]. However, other (time-independent) formulations do exist. For example, in ensemble DFT (EDFT), one describes the electron density by an ensemble of densities made of several states rather than a single density as in traditional DFT. In the context of excited states, EDFT was first introduced by Theophilou [11] based on equally-weighted ensembles followed by the Gross-Oliviera-Kohn generalization for unequally-weighted ensembles [12–14]. In recent times, EDFT has undergone significant developments that are crucial to its advancement [15–33].

Concerning pure excited states, orbital-optimized DFT [34–45] has been shown to be relatively successful for certain classes of excited states, such as doubly-excited and charge-transfer states [38, 39] (see also Ref. 46).

From a more theoretical point of view, based on the work of Levy and Nagy on a constrained search for excited states [47], Ayers *et al.* reported, in a series of papers, a generalization of the ground-state formalism, for Coulombic systems, to pure excited states [48–50]. The first paper of this series highlights the unique features of the Coulombic Hamiltonian that determines not only the Hamiltonian but also the degree of excitation [48]. The second paper deals with the generalization of the Kohn-Sham scheme to this new theory [49], while the third and final paper of the series reports a generalization to subspaces [50]. Therefore, although there is, in general, a lack of Hohenberg-Kohn theorem for excited states (*i.e.*, there is no one-to-one mapping between the excited state density and the external potential) [51], in the context of molecules, it is possible to identify excited states directly from their density, which enables the construction of exact DFT functionals for individual excited states (see also Ref. 52).

Here, we show that, for the simple asymmetric Hubbard dimer at half-filling, it is possible to determine the exact density functional for each singlet excited state by seeking — via a straightforward generalization of Levy’s constrained search or Lieb’s convex formulation — all the stationary points associated with Eq. (6) or Eq. (2). However, as we shall see below, the “functional” associated with the first excited state has some very peculiar mathematical properties.

*The asymmetric Hubbard dimer.* — The Hamiltonian of the asymmetric Hubbard dimer is [53, 54]

$$\hat{H} = -t \sum_{\sigma=\uparrow,\downarrow} (a_{0\sigma}^\dagger a_{1\sigma} + \text{h.c.}) + U \sum_{i=0}^1 \hat{n}_{i\uparrow} \hat{n}_{i\downarrow} + \Delta v \frac{\hat{n}_1 - \hat{n}_0}{2} \quad (9)$$

where  $t > 0$  is the hopping parameter,  $U \geq 0$  is the on-site interaction parameter,  $\hat{n}_{i\sigma} = a_{i\sigma}^\dagger a_{i\sigma}$  is the spin density operator on site  $i$ ,  $\hat{n}_i = \hat{n}_{i\uparrow} + \hat{n}_{i\downarrow}$  is the density operator on site  $i$ , and  $\Delta v = v_1 - v_0$  (with  $v_0 + v_1 = 0$ ) is the potential difference between the two sites.

At half filling ( $N = 2$ ), we expand the Hamiltonian in the  $N$ -electron (spin-adapted) site basis  $|0_\uparrow 0_\downarrow\rangle$ ,  $(|0_\uparrow 1_\downarrow\rangle - |0_\downarrow 1_\uparrow\rangle)/\sqrt{2}$ , and  $|1_\uparrow 1_\downarrow\rangle$  to form the following Hamiltonian matrix

$$\mathbf{H} = \begin{pmatrix} U - \Delta v & -\sqrt{2}t & 0 \\ -\sqrt{2}t & 0 & -\sqrt{2}t \\ 0 & -\sqrt{2}t & U + \Delta v \end{pmatrix} \quad (10)$$

which eigenvalues provide the singlet energies of the system. A generic singlet wave function can then be written as

$$|\Psi\rangle = x |0_\uparrow 0_\downarrow\rangle + y \frac{|0_\uparrow 1_\downarrow\rangle - |0_\downarrow 1_\uparrow\rangle}{\sqrt{2}} + z |1_\uparrow 1_\downarrow\rangle \quad (11)$$

with  $-1 \leq x, y, z \leq 1$  and the normalization condition

$$x^2 + y^2 + z^2 = 1 \quad (12)$$

The energy is given by

$$E = T + V_{ee} + V \quad (13)$$

with

$$T = -2\sqrt{2}ty(x+z) \quad (14a)$$

$$V_{ee} = U(x^2 + z^2) \quad (14b)$$

$$V = \frac{\Delta v \Delta n}{2} = \Delta v(z^2 - x^2), \quad (14c)$$

and  $\Delta n = \langle \hat{n}_1 - \hat{n}_0 \rangle$ .

In the following, we call  $E_0$ ,  $E_1$ , and  $E_2$  the energies of the ground state, first (singly-)excited state, and second (doubly-)excited state, respectively. These are represented in Fig. 1 as functions of  $\Delta v$  for  $t = 1/2$  and  $U = 1$ . It is worth noting that  $E_0$  (left panel) and  $E_2$  (right panel) are concave and convex with respect to  $\Delta v$ , respectively, for any value of  $t$  and  $U$ , while  $E_1$  (central panel) is concave for  $\Delta v$  smaller than a critical value  $\Delta v_c$  (blue curve labeled as  $E_1^\cap$ ) and becomes convex for  $\Delta v > \Delta v_c$  (yellow curve labeled as  $E_1^\cup$ ).

The corresponding differences in (reduced) site occupation

$$\rho = \frac{\Delta n}{2} \quad (15)$$

for the ground state,  $\rho_0$ , first (singly-)excited state,  $\rho_1$ , and second (doubly-)excited state,  $\rho_2$ , are represented in Fig. 2. While the ground (red curve) and the doubly-excited (green curve) states have monotonic densities with respect to  $\Delta v$  for any  $t$  and  $U$  values,  $\rho_1$  is non-monotonic and reaches a critical value  $\rho_c$  at  $\Delta v_c$  before decaying to 0 as  $\Delta v \rightarrow \infty$ .

*Levy’s constrained search.* — Substituting  $x$  and  $z$  in Eqs. (14a) and (14b) thanks to the normalization condition defined in Eq. (12) and the reduced site occupation difference

$$\rho = z^2 - x^2 \quad (16)$$

we obtain the four-branch function

$$f_{\pm\pm}(\rho, y) = -2ty \left( \pm\sqrt{1-y^2-\rho} \pm \sqrt{1-y^2+\rho} \right) + U(1-y^2) \quad (17)$$

that one would minimize with respect to  $y$  to obtain the exact ground-state functional [53, 55]. (Although one technically deals with *functions* in the Hubbard dimer, we shall stick to the term *functional* to emphasize the formal analogy between site-occupation function theory and DFT, as customarily done in the literature [55–58].)

Rather than only minimizing Eq. (17) for a given  $\rho$ , we seek *all* stationary points of  $f_{\pm\pm}(\rho, y)$  with respect to  $y$ , *i.e.*,

$$\frac{\partial f_{\pm\pm}(\rho, y)}{\partial y} = 0 \quad (18)$$

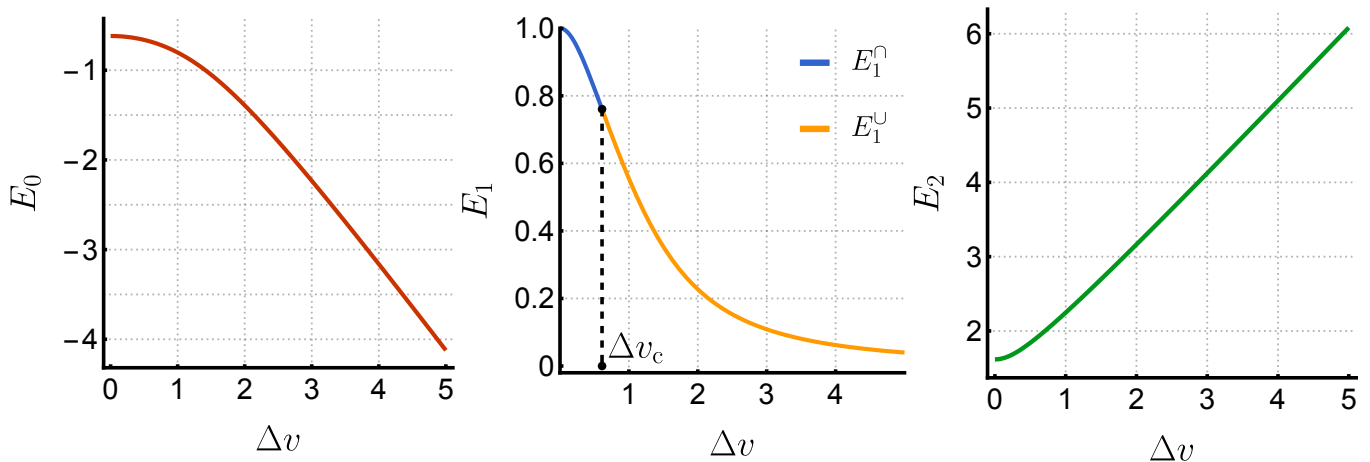


FIG. 1.  $E_0$  (left),  $E_1$  (center), and  $E_2$  (right) as functions of  $\Delta v$  for  $t = 1/2$  and  $U = 1$ . Note that  $E$  is an even function of  $\Delta v$ .  $E_1$  is concave  $\Delta v < \Delta v_c$  and becomes convex for larger  $\Delta v$  values.

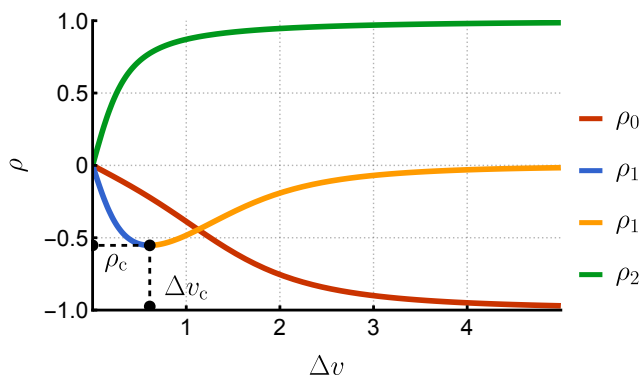


FIG. 2.  $\rho$  as a function of  $\Delta v$  for  $t = 1/2$  and  $U = 1$  for the ground state ( $\rho_0$ ), the singly-excited state ( $\rho_1$ ), and the doubly-excited states ( $\rho_2$ ).  $\rho_1$  reaches a critical value,  $\rho_c$ , at  $\Delta v_c$ . Note that  $\rho$  is an odd function of  $\Delta v$ .

Note that the choice of the minimizing variable  $y$  in Eq. (17) is arbitrary and various other choices are possible yielding different functions than  $f_{\pm\pm}$  [53], yet identical exact density functionals.

Because  $f_{\pm\pm}$  is an even function of  $y$ , we restrict the discussion to the domain where  $y \geq 0$ , without loss of generalities. As depicted in Fig. 3, the branches  $f_{++}$  and  $f_{--}$  have one stationary point each for  $y \geq 0$  (green square and red circle, respectively): the global minimum located at  $y_0$  corresponds to the convex ground-state functional,  $F_0(\rho) = f_{++}(\rho, y_0)$ , while the global maximum at  $y_2$  corresponds to the concave doubly-excited-state functional, *i.e.*,  $F_2(\rho) = f_{--}(\rho, y_2)$  (see Fig. 4).  $F_0(\rho)$  and  $F_2(\rho)$  merge at  $\rho = 1$ . The stationary points located at  $-y_0$  and  $-y_2$  are associated with opposite values of  $\Delta v$ .

For  $\rho < \rho_c$ , the branch  $f_{+-}$  has two stationary points (yellow diamonds): a local minimum at  $y_1^\cap$  and a local

maximum at  $y_1^\cup$  that yield a concave branch  $F_1^\cap(\rho) = f_{+-}(\rho, y_1^\cap)$  (yellow curve in Fig. 4) and a convex branch  $F_1^\cup(\rho) = f_{+-}(\rho, y_1^\cup)$  (blue curve in Fig. 4) for the singly-excited-state functional. As expected though,  $F_1^\cap(\rho)$  and  $F_1^\cup(\rho)$  lead to convex and concave energies,  $E_1^\cup$  and  $E_1^\cap$  (see Fig. 1), respectively, preserving the property that the energy and the functional are conjugate functions [6]. Because the density of the first excited state is non-invertible, its “functional” is a partial (*i.e.*, defined for a subdomain of  $\rho$ ), multi-valued function constituted of one concave and one convex branch that correspond to two separate sets of values of the external potential. Again, the stationary points on  $f_{+-}$  located at  $-y_1^\cap$  and  $-y_1^\cup$  (blue triangles) are associated with opposite values of  $\Delta v$ . At  $\rho = \rho_c$ ,  $y_1^\cap$  and  $y_1^\cup$  merge and disappear for larger  $\rho$  values. This critical value of the density decreases with respect to  $U$  to reach zero at  $U = 0$ , and  $\rho_c \rightarrow 1$  as  $U \rightarrow \infty$ .

In accordance with Eq. (7), the derivative of  $F_0(\rho)$  with respect to  $\rho$  gives back  $\Delta v_0$  as a function of  $\rho$ , *i.e.*, the inverse of  $\rho_0(\Delta v)$  plotted in Fig. 2. Most notably, an analogous relation holds for the excited states. For the doubly-excited state, we simply have

$$\frac{dF_2(\rho)}{d\rho} = -\Delta v_2(\rho) \quad (19)$$

In particular, for  $\rho = 0$ , we have  $\Delta v_2 = 0$ , while  $\Delta v_2 \rightarrow \infty$  as  $\rho \rightarrow 1$ , similarly to  $\Delta v_0$  (except that  $\Delta v_0 \rightarrow -\infty$  as  $\rho \rightarrow 1$ ).

For the first excited state, which has a non-invertible density,  $\rho_1(\Delta v)$  (see Fig. 2), we still have

$$\frac{dF_1^\cup(\rho)}{d\rho} = -\Delta v_1^\cup(\rho) \quad (20a)$$

$$\frac{dF_1^\cap(\rho)}{d\rho} = -\Delta v_1^\cap(\rho) \quad (20b)$$

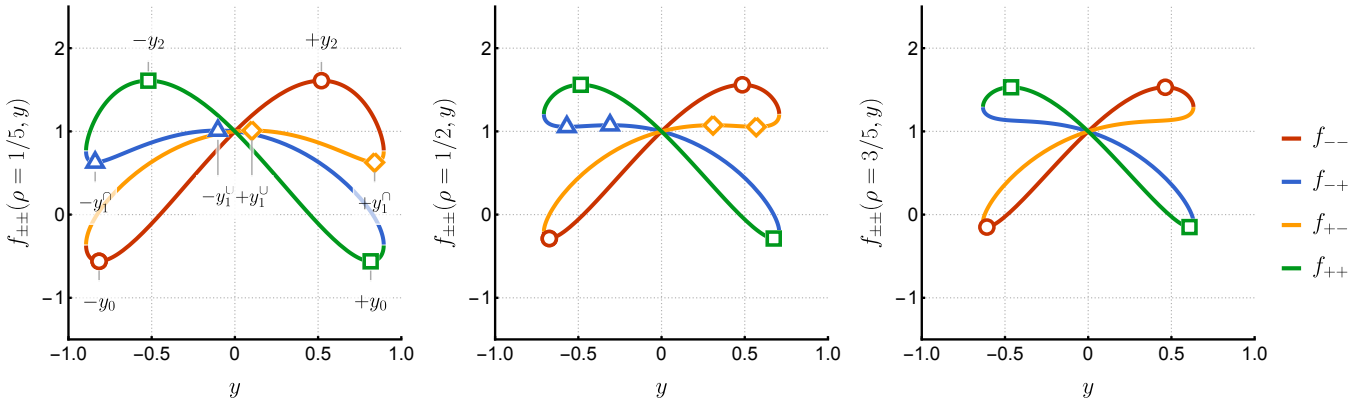


FIG. 3.  $f_{--}(\rho, y)$  (red),  $f_{-+}(\rho, y)$  (blue),  $f_{+-}(\rho, y)$  (yellow), and  $f_{++}(\rho, y)$  (green) as functions of  $y$  for  $t = 1/2$ ,  $U = 1$ , and  $\rho = 1/5$  (left),  $1/2$  (center), and  $3/5$  (right). The markers indicate the position of the stationary points on each branch. At  $\rho = 3/5$  (right panel), the stationary points of  $f_{-+}$  and  $f_{+-}$  have disappeared as  $\rho > \rho_c$  (see Fig. 2).

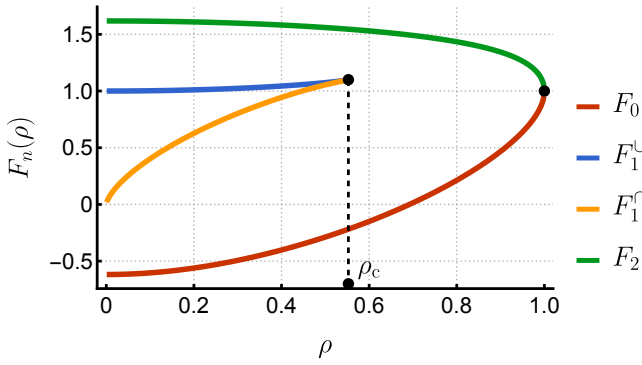


FIG. 4. State-specific exact functionals  $F_n(\rho)$  as functions of  $\rho$  for  $t = 1/2$  and  $U = 1$ . The ground-state functional  $F_0(\rho)$  (red) is concave with respect to  $\rho$ , the singly-excited state multi-valued functional  $F_1(\rho)$  has one concave branch (blue) and one convex branch (yellow), each associated with a separate set of  $\Delta v$  values, while the doubly-excited state functional  $F_2(\rho)$  (green) is convex. Note that  $F$  is an even function of  $\rho$ .

where  $\Delta v_1^U(\rho)$  ranges from  $-\Delta v_c$  (at  $\rho = \rho_c$ ) to 0 (for  $\rho = 0$ ), yielding the inverse of the blue curve in Fig. 2, and  $\Delta v_1^\cap(\rho)$  ranges from  $-\infty$  (for  $\rho = 0$ ) to  $-\Delta v_c$  (for  $\rho = \rho_c$ ), yielding the inverse of the yellow curve in Fig. 2.

The Levy constrained-search procedure producing these exact functionals is geometrically illustrated in Fig. 5. The surface of the (unit) sphere corresponds to the normalized wave functions such that  $x^2 + y^2 + z^2 = 1$ , onto which we have mapped the value of  $T + V_{ee}$  as a function of  $x$ ,  $y$ , and  $z$ . The gray parabolas correspond to the (potentially unnormalized) wave functions yielding  $\rho = z^2 - x^2$ . Hence, the contours obtained by the intersection of these three-dimensional surfaces are the normalized wave functions yielding  $\rho = z^2 - x^2$ . On these contours, one is looking for the points where  $f_{\pm\pm}$  is stationary. These are represented by the colored dots in

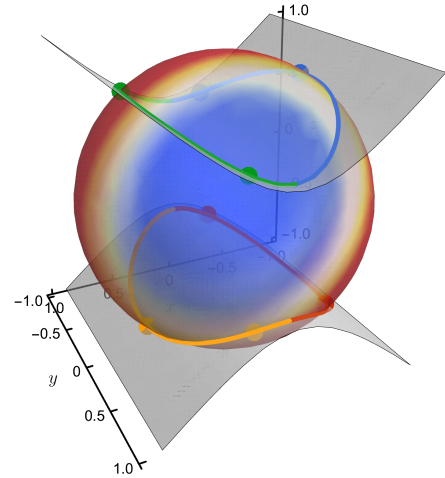


FIG. 5. Illustration of the Levy constrained-search procedure for  $t = 1/2$ ,  $U = 1$ , and  $\rho = 1/5$ . The value of  $T + V_{ee}$  is mapped on the surface of the unit sphere that represents the normalized wave functions. The gray parabolas correspond to densities  $\rho = z^2 - x^2$ . The four branches of  $f_{\pm\pm}$  [see Eq. (17)] are represented as contours and corresponds to the intersections of these three-dimensional objects. The dots locate the stationary points on each of these contours.

Fig. 5 (see also Fig. 3).

*Lieb's convex formulation.*— The exact functionals represented in Fig. 4 can also be obtained using the Lieb variational principle. To do so, let us define, for each singlet state, the following function

$$f_n(\rho, \Delta v) = E_n - \Delta v \rho \quad (21)$$

However, instead of maximizing the previous expression for a given  $\rho$  as in Eq. (2), we seek its entire set of stationary points with respect to  $\Delta v$  for each  $n$  value, *i.e.*

$$\frac{\partial f_n(\rho, \Delta v)}{\partial \Delta v} = 0 \quad (22)$$

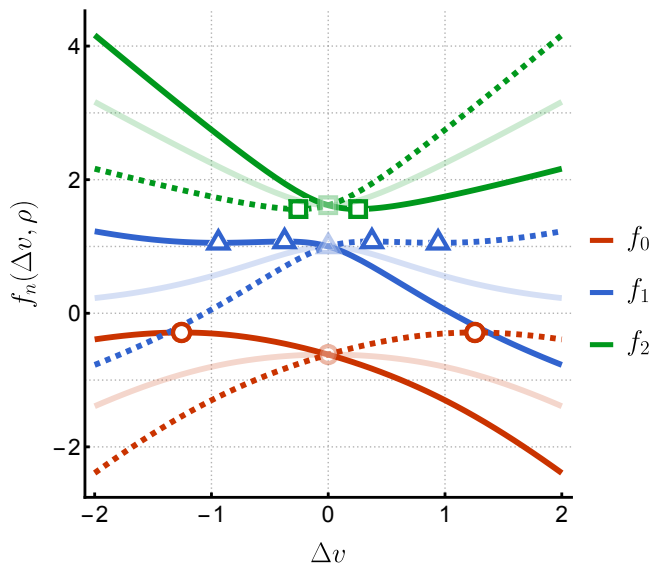


FIG. 6.  $f_n(\rho, \Delta v)$  as a function of  $\Delta v$  for  $t = 1/2$ ,  $U = 1$ , and  $\rho = \pm 1/2$ : ground state ( $n = 0$ ), singly-excited state ( $n = 1$ ), and doubly-excited state ( $n = 2$ ). The markers indicate the position of the stationary points. The transparent curves correspond to  $\rho = 0$ . In this case, the linear term  $-\Delta v \rho$  in Eq. (2) vanishes and the energy  $E_n$  is recovered (see Fig. 1). For  $\rho = 1/2$  (solid curves), the linear term shifts the maxima of  $E_0$  and  $E_1$  (red circle and blue triangle, respectively) towards  $\Delta v < 0$  and the minimum of  $E_2$  (green square) towards  $\Delta v > 0$ . Moreover, a local minimum in  $f_1$  (outermost blue triangle) appears. For  $\rho = -1/2$  (dashed curves) the situation is exactly mirrored.

Figure 6 shows  $f_n$  as a function of  $\Delta v$  at  $\rho = 0$  and  $\pm 1/2$  for each state and the location of the corresponding stationary points. For  $\rho = 0$  (transparent curves), one recovers the energies  $E_n$  plotted in Fig. (1). The values of the functions  $f_n$  at their stationary points (red circle, blue triangle, and green square at  $\Delta v = 0$ ) correspond to the initial values of  $F_0$ ,  $F_1^\cup$ , and  $F_2$  in Fig 4. For  $\rho = 1/2$ ,  $f_0$  (solid red curve) and  $f_2$  (solid green curve) have a single extremum: a maximum and a minimum yielding the ground-state and second-excited-state functionals,  $F_0(\rho)$  and  $F_2(\rho)$ , respectively, as depicted in Fig. 4. The blue curve  $f_1$  exhibits a local maximum and minimum that corresponds to the two branches of the multi-valued functional associated with the first excited state,  $F_1^\cap(\rho)$  and  $F_1^\cup(\rho)$ , respectively.

In practice, Lieb’s formulation has a very neat geometric illustration in the Hubbard dimer: the total energies  $E_n$  are “tipped” by the addition of the linear term  $-\Delta v \rho$ , which shifts their extrema: the maxima of  $E_0$  and  $E_1$  towards  $\Delta v < 0$  and the minimum of  $E_2$  towards  $\Delta v > 0$ . Moreover, in the case of the first excited state, the linear curve  $-\Delta v \rho$  shifts the energy in such a way that, as soon as  $\rho > 0$ , a local minimum appears (outermost blue triangle) in  $f_1$ . This minimum and maximum gradually get closer as  $\rho$  increases, until they merge at  $\rho = \rho_c$ ,  $f_1$

becoming monotonic with no stationary points for  $\rho > \rho_c$ . For  $\rho = -1/2$  (dashed curves) the situation is exactly mirrored.

*Conclusion.*— The present Letter reports the exact functional for the ground and the (singlet) excited states of the asymmetric Hubbard dimer at half-filling. To the best of our knowledge, this is the first time that exact function(al)s corresponding to singlet (non-degenerate) excited states are computed. While the ground-state functional is well-known to be a convex function with respect to the difference in site occupations, the functional associated with the highest doubly-excited state is found to be concave. Additionally, and more importantly, we discovered that the “functional” for the first excited state is a partial, multi-valued function of the density that is constructed from one concave and one convex branch associated with two separate sets of values of the external potential. Furthermore, we find that Levy’s constrained search and Lieb’s convex formulation are entirely consistent for all the states of the model, producing the same landscape of state-specific functionals. These findings may provide insight into the challenges of constructing state-specific excited-state density functionals for general applications in electronic structure theory.

*Acknowledgements.*— This project has received funding from the European Research Council (ERC) under the European Union’s Horizon 2020 research and innovation programme (Grant agreement No. 863481).

\* [sgiarrosso@irsamc.ups-tlse.fr](mailto:sgiarrosso@irsamc.ups-tlse.fr)

† [loos@irsamc.ups-tlse.fr](mailto:loos@irsamc.ups-tlse.fr)

- [1] A. M. Teale, T. Helgaker, A. Savin, C. Adamo, B. Aradi, A. V. Arbuznikov, P. W. Ayers, E. J. Baerends, V. Barone, P. Calaminici, E. Cancès, E. A. Carter, P. K. Chattaraj, H. Chermette, I. Ciofini, T. D. Crawford, F. De Proft, J. F. Dobson, C. Draxl, T. Frauenheim, E. Fromager, P. Fuentealba, L. Gagliardi, G. Galli, J. Gao, P. Geerlings, N. Gidopoulos, P. M. W. Gill, P. Gori-Giorgi, A. Görling, T. Gould, S. Grimme, O. Gritsenko, H. J. A. Jensen, E. R. Johnson, R. O. Jones, M. Kaupp, A. M. Köster, L. Kronik, A. I. Krylov, S. Kvaal, A. Laestadius, M. Levy, M. Lewin, S. Liu, P.-F. Loos, N. T. Maitra, F. Neese, J. P. Perdew, K. Pernal, P. Pernot, P. Piecuch, E. Rebolini, L. Reining, P. Romaniello, A. Ruzsinszky, D. R. Salahub, M. Scheffler, P. Schwerdtfeger, V. N. Staroverov, J. Sun, E. Tellgren, D. J. Tozer, S. B. Trickey, C. A. Ullrich, A. Vela, G. Vignale, T. A. Wesolowski, X. Xu, and W. Yang, *Phys. Chem. Chem. Phys.* **24**, 28700 (2022).
- [2] P. Hohenberg and W. Kohn, *Phys. Rev.* **136**, B864 (1964).
- [3] W. Kohn and L. J. Sham, *Phys. Rev.* **140**, A1133 (1965).
- [4] M. Levy, *Proc. Natl. Acad. Sci. U.S.A.* **76**, 6062 (1979).
- [5] E. H. Lieb, *Int. J. Quantum Chem.* **24**, 243 (1983).
- [6] T. Helgaker and A. M. Teale, in *The Physics and Mathematics of Elliott Lieb* (EMS Press, 2022) pp. 527–559.
- [7] E. Runge and E. K. U. Gross, *Phys. Rev. Lett.* **52**, 997 (1984).

- [8] K. Burke, J. Werschnik, and E. K. U. Gross, *J. Chem. Phys.* **123**, 062206 (2005).
- [9] M. Casida and M. Huix-Rotllant, *Annu. Rev. Phys. Chem.* **63**, 287 (2012).
- [10] M. Huix-Rotllant, N. Ferré, and M. Barbatti, “Time-dependent density functional theory,” in *Quantum Chemistry and Dynamics of Excited States* (John Wiley & Sons, Ltd, 2020) Chap. 2, pp. 13–46.
- [11] A. K. Theophilou, *J. Phys. C* **12**, 5419 (1979).
- [12] E. K. U. Gross, L. N. Oliveira, and W. Kohn, *Phys. Rev. A* **37**, 2805 (1988).
- [13] E. K. U. Gross, L. N. Oliveira, and W. Kohn, *Phys. Rev. A* **37**, 2809 (1988).
- [14] E. K. U. Gross, L. N. Oliveira, and W. Kohn, *Phys. Rev. A* **37**, 2805 (1988).
- [15] A. Pribram-Jones, Z.-h. Yang, J. R. Trail, K. Burke, R. J. Needs, and C. A. Ullrich, *J. Chem. Phys.* **140**, 18A541 (2014).
- [16] Z.-H. Yang, J. R. Trail, A. Pribram-Jones, K. Burke, R. J. Needs, and C. A. Ullrich, *Phys. Rev. A* **90**, 042501 (2014).
- [17] B. Senjean, S. Knecht, H. J. A. Jensen, and E. Fromager, *Phys. Rev. A* **92**, 012518 (2015).
- [18] M. Filatov, “Ensemble DFT Approach to Excited States of Strongly Correlated Molecular Systems,” in *Density-Functional Methods for Excited States*, edited by N. Ferré, M. Filatov, and M. Huix-Rotllant (Springer International Publishing, Cham, 2016) pp. 97–124.
- [19] T. Gould and S. Pittalis, *Phys. Rev. Lett.* **119**, 243001 (2017).
- [20] Z.-H. Yang, A. Pribram-Jones, K. Burke, and C. A. Ullrich, *Phys. Rev. Lett.* **119**, 033003 (2017).
- [21] K. Deur, L. Mazouin, and E. Fromager, *Phys. Rev. B* **95**, 035120 (2017).
- [22] F. Sagredo and K. Burke, *J. Chem. Phys.* **149**, 134103 (2018).
- [23] T. Gould, L. Kronik, and S. Pittalis, *J. Chem. Phys.* **148**, 174101 (2018).
- [24] T. Gould and S. Pittalis, *Phys. Rev. Lett.* **123**, 016401 (2019).
- [25] K. Deur and E. Fromager, *J. Chem. Phys.* **150**, 094106 (2019).
- [26] T. Gould, G. Stefanucci, and S. Pittalis, *Phys. Rev. Lett.* **125**, 233001 (2020).
- [27] C. Marut, B. Senjean, E. Fromager, and P.-F. Loos, *Faraday Discuss.* **224**, 402 (2020).
- [28] P.-F. Loos and E. Fromager, *J. Chem. Phys.* **152**, 214101 (2020).
- [29] E. Fromager, *Phys. Rev. Lett.* **124**, 243001 (2020).
- [30] T. Gould, L. Kronik, and S. Pittalis, *Phys. Rev. A* **104**, 022803 (2021).
- [31] F. Cernatic, B. Senjean, V. Robert, and E. Fromager, *Top. Curr. Chem.* **380**, 1 (2022).
- [32] T. Gould, Z. Hashimi, L. Kronik, and S. G. Dale, *J. Phys. Chem. Lett.* **13**, 2452 (2022).
- [33] T. Gould, D. P. Kooi, P. Gori-Giorgi, and S. Pittalis, *Phys. Rev. Lett.* **130**, 106401 (2023).
- [34] T. Kowalczyk, T. Tsuchimochi, P.-T. Chen, L. Top, and T. Van Voorhis, *J. Chem. Phys.* **138**, 164101 (2013).
- [35] A. T. Gilbert, N. A. Besley, and P. M. Gill, *J. Phys. Chem. A* **112**, 13164 (2008).
- [36] G. M. J. Barca, A. T. B. Gilbert, and P. M. W. Gill, *J. Chem. Theory Comput.* **14**, 1501 (2018).
- [37] G. M. J. Barca, A. T. B. Gilbert, and P. M. W. Gill, *J. Chem. Theory Comput.* **14**, 9 (2018).
- [38] D. Hait and M. Head-Gordon, *J. Chem. Theory Comput.* **16**, 1699 (2020).
- [39] D. Hait and M. Head-Gordon, *J. Phys. Chem. Lett.* **12**, 4517 (2021).
- [40] J. A. R. Shea and E. Neuscamman, *J. Chem. Phys.* **149**, 081101 (2018).
- [41] J. A. R. Shea, E. Gwin, and E. Neuscamman, *J. Chem. Theory Comput.* **16**, 1526 (2020).
- [42] T. S. Hardikar and E. Neuscamman, *J. Chem. Phys.* **153**, 164108 (2020).
- [43] G. Levi, A. V. Ivanov, and H. Jónsson, *J. Chem. Theory Comput.* **16**, 6968 (2020).
- [44] K. Carter-Fenk and J. M. Herbert, *J. Chem. Theory Comput.* **16**, 5067 (2020).
- [45] D. Toffoli, M. Quarin, G. Fronzoni, and M. Stener, *J. Phys. Chem. A* **126**, 7137 (2022).
- [46] J. P. Perdew and M. Levy, *Phys. Rev. B* **31**, 6264 (1985).
- [47] M. Levy and A. Nagy, *Phys. Rev. Lett.* **83**, 4361 (1999).
- [48] P. W. Ayers, M. Levy, and A. Nagy, *Phys. Rev. A* **85**, 042518 (2012).
- [49] P. W. Ayers, M. Levy, and Á. Nagy, *J. Chem. Phys.* **143**, 191101 (2015).
- [50] P. W. Ayers, M. Levy, and A. Nagy, *Theor. Chem. Acc.* , 137 (2018).
- [51] R. Gaudoin and K. Burke, *Phys. Rev. Lett.* **93**, 173001 (2004).
- [52] L. Garrigue, *Arch. Rational Mech. Anal.* **245**, 949 (2022).
- [53] D. J. Carrascal, J. Ferrer, J. C. Smith, and K. Burke, *J. Phys. Condens. Matter* **27**, 393001 (2015).
- [54] D. J. Carrascal, J. Ferrer, N. Maitra, and K. Burke, *Eur. Phys. J. B* **91**, 142 (2018).
- [55] A. J. Cohen and P. Mori-Sánchez, *Phys. Rev. A* **93**, 042511 (2016).
- [56] K. Capelle and V. L. Campo Jr, *Phys. Rep.* **528**, 91 (2013).
- [57] T. Dimitrov, H. Appel, J. I. Fuks, and A. Rubio, *New J. Phys.* **18**, 083004 (2016).
- [58] B. Senjean, M. Tsuchiizu, V. Robert, and E. Fromager, *Mol. Phys.* **115**, 48 (2017).